BMC Developmental Biology

BioMed Central

Research article

Late gestational lung hypoplasia in a mouse model of the Smith-Lemli-Opitz syndrome

Hongwei Yu*[1], Andy Wessels[2], Jianliang Chen[1], Aimee L Phelps[2], John Oatis[1], G Stephen Tint[3] and Shailendra B Patel[1]

Address: [1]Division of Endocrinology, Diabetes and Medical Genetics, Medical University of South Carolina, STR 541, 114 Doughty Street, Charleston, SC 29403, USA, [2]Department of Cell Biology and Anatomy, Medical University of South Carolina, Charleston, SC 29403, USA and [3]Research Service, Department of Veterans Affairs New Jersey Health Care System, East Orange, NJ, USA and Medical Service, UMDNJ-New Jersey Medical School, Newark, NJ, USA

Email: Hongwei Yu* - yuh@musc.edu; Andy Wessels - wesselsa@musc.edu; Jianliang Chen - chenjl@musc.edu; Aimee L Phelps - phelpsal@musc.edu; John Oatis - oatisje@musc.edu; G Stephen Tint - tintgs@umdnj.edu; Shailendra B Patel - patelsb@musc.edu

* Corresponding author

Published: 02 February 2004

BMC Developmental Biology 2004, **4**:1

Received: 07 October 2003
Accepted: 02 February 2004

This article is available from: http://www.biomedcentral.com/1471-213X/4/1

Abstract

Background: Normal post-squalene cholesterol biosynthesis is important for mammalian embryonic development. Neonatal mice lacking functional dehydrocholesterol Δ7-reductase (Dhcr7), a model for the human disease of Smith-Lemli-Opitz syndrome, die within 24 hours of birth. Although they have a number of biochemical and structural abnormalities, one cause of death is from apparent respiratory failure due to developmental pulmonary abnormalities.

Results: In this study, we characterized further the role of cholesterol deficiency in lung development of these mice. Significant growth retardation, beginning at E14.5~E16.5, was observed in *Dhcr7*$^{-/-}$ embryos. Normal lobation but smaller lungs with a significant decrease in lung-to-body weight ratio was noted in *Dhcr7*$^{-/-}$ embryos, compared to controls. Lung branching morphogenesis was comparable between *Dhcr7*$^{-/-}$ and controls at early stages, but delayed saccular development was visible in all *Dhcr7*$^{-/-}$ embryos from E17.5 onwards. Impaired pre-alveolar development of varying severity, inhibited cell proliferation, delayed differentiation of type I alveolar epithelial cells (AECs) and delayed vascular development were all evident in knockout lungs. Differentiation of type II AECs was apparently normal as judged by surfactant protein (SP) mRNAs and SP-C immunostaining. A significant amount of cholesterol was detectable in knockout lungs, implicating some maternal transfer of cholesterol. No significant differences of the spatial-temporal localization of sonic hedgehog (Shh) or its downstream targets by immunohistochemistry were detected between knockout and wild-type lungs and Shh autoprocessing occurred normally in tissues from *Dhcr7*$^{-/-}$ embryos.

Conclusion: Our data indicated that cholesterol deficiency caused by *Dhcr7* null was associated with a distinct lung saccular hypoplasia, characterized by failure to terminally differentiate alveolar sacs, a delayed differentiation of type I AECs and an immature vascular network at late gestational stages. The molecular mechanism of impaired lung development associated with sterol deficiency by *Dhcr7* loss is still unknown, but these results do not support the involvement of dysregulated Shh-Patched-Gli pathway in causing this defect.

Background

Cholesterol is a necessary membrane constituent of all mammalian, reptile and avian cells, as well as a few other organisms, but not all eukaryotic organisms. In the latter cases, such as plants and fungi, cholesterol-like sterols (phytosterols, ergosterol etc.) seem to substitute for cholesterol. The precise need for sterols in biological membranes still remains poorly defined, though its link with microdomains (variously termed rafts, caveoli etc.) may be part of the answer [1]. Although the accumulation of cholesterol in atherosclerotic plaques has led to the concept that 'too much' cholesterol may be deleterious, too little cholesterol has now been proven pathophysiological for abnormal embryonic development. Smith-Lemli-Opitz syndrome (SLOS, MIM 270400), a relative common dysmorphology disorder, is caused by mutations in DHCR7 [2-5], which encodes for 7-dehydrocholesterol Δ7-reductase and catalyzes a final step of cholesterol biosynthesis. Recognition of other dysmorphology syndromes caused by defects in the post-squalene cholesterol biosynthesis pathway, such as desmosterolosis, lathosterolosis, X-linked chondrodysplasia punctanta and CHILD syndrome [6-15], has strengthened this concept.

Genetic disruption of the *Dhcr7* results in neonatal lethality [16]. Neonatal mice homozygous for the *Dhcr7* gene disruption are deficient in cholesterol and have increased accumulation of the cholesterol precursor 7-dehydrocholesterol (7DHC). Although no embryonic lethality was noted, these knockout pups exhibited a number of developmental abnormalities and died within 24 h after birth. A similar mouse SLOS model, generated by replacing exons 3, 4 and part of exon 5 of the murine *Dhcr7* gene, with similar biochemical and structural defects and a 100 % neonatal lethality, has also been reported [17]. Poor lung development or diffuse lung alveolar atelectasis with cyanotic and lethargic breathing are consistent between both *Dhcr7* null models [16,17], and therefore is the likely reason for the respiratory insufficiency and subsequent death of *Dhcr7*$^{-/-}$ pups. These *Dhcr7* knockout mice are models for human SLOS, especially the more severely affected patients, since early postnatal lethality with respiratory failure has been reported in severe SLOS cases [4,5]. Developmental lung abnormalities are also relatively common in SLOS patients, including pulmonary hypoplasia, abnormal pulmonary lobation and pulmonary arteries, anomalies of laryngeal and tracheal development [18].

Mammalian lung is unique in that it is fully developed, but does not function for gas exchange until at the moment of birth; the majority of structural development and maturation takes place *in utero*. Lung development is a complex process that involves branching morphogenesis of epithelium, interstitial development including vasculogenesis, cellular differentiation, biochemical maturation and physical growth. Four stages of mouse lung development have been described, based upon the histological appearances of lung; pseudoglandular, canalicular, terminal saccular and alveolar stages [19].

Impaired hedgehog function has been proposed as a mechanism underlying malformations found in SLOS. Hedgehog family members play diverse roles in embryonic development, and cholesterol is necessary for maturation of these morphogens [20-23]. The sonic hedgehog (Shh) signaling cascade has been shown to play a central role in lung development [24-26]. Loss of Shh function resulted in severe lung defects associated with loss of branching morphogenesis, but preserved proximal-to-distal differentiation of lung epithelium [24]. Overexpression of Shh in the distal lung epithelium resulted in the absence of functional alveoli and an increase in interstitial tissue caused by an increased proliferation of both epithelial and mesenchyme cells [26]. Mice with Shh overexpression died less than 24 h after birth, probably owing to respiratory failure. It has been reported that inhibition of cholesterol biosynthesis by chemical inhibitors of *Dhcr7* also led to a disturbance of the Shh signaling with abnormal embryogenesis [27,28], and severe sterol deprivation can indeed inhibit the processing of transfected Shh in cultured mammalian cells [29].

In the present studies, we characterized lung development in *Dhcr7*$^{-/-}$ embryos from E10.5 to birth. Our results showed that cholesterol deficiency, caused by loss of Dhcr7 activity, did not alter lung branching morphogenesis (early gestational stages, E9.5 to E14.5). However, lung saccular development was impaired, with arrested or partially developed epithelial tubules and delayed vascular development. Differentiation of type II alveolar epithelial cells (AECs) appeared normal but differentiation of type I AECs was severely impaired. Therefore, cholesterol deficiency resulted in a distinct late gestational lung hypoplasia, characterized by impaired sacculation with delayed type I AECs differentiation and immature vascular development. However, this study does not support the concept that the perturbation of Shh-Patched-Gli pathway was involved in the pathogenesis of developmental lung hypoplasia in *Dhcr7*$^{-/-}$ embryos. Patterns of expression of Shh signaling cascade members were not altered, and processing of Shh appeared normal.

Results

Body growth retardation at late gestation stage in Dhcr7$^{-/-}$ *embryos*

Dhcr7$^{-/-}$ mice were born in the expected Mendelian ratios from heterozygous parents, but all of these pups died within 24 h and most within 14 h of birth [16]. At birth, they were clearly smaller than wild-type or heterozygous

Table 1: Whole body and lung weights of mouse embryos

	E13.5		E18.5	
	Dhcr7$^{+/+}$	*Dhcr7*$^{-/-}$	*Dhcr7*$^{+/+}$	*Dhcr7*$^{-/-}$
N	10	4	17	8
Wet BW (mg)	142 ± 0.21	138 ± 11	1015.3 ± 12	825.7 ± 14 *
Wet LW (mg)	8.1 ± 0.21	8.0 ± 0.4	43.44 ± 8.96	33.96 ± 11.37 *
LW/BW ratio (%)	5.7 ± 0.54	5.81 ± 0.55	4.4 ± 0.6	3.84 ± 0.63 *

* $p < 0.05$, compared to *Dhcr7*$^{+/+}$. BW, body weight; LW, lung weight.

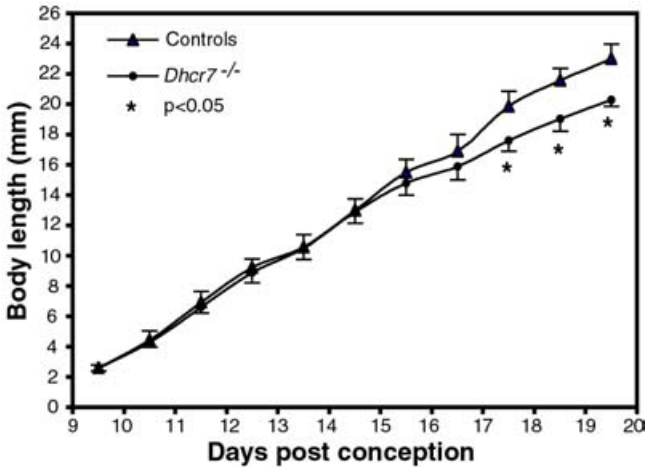

Figure 1

Body length growth curves. Body length growth *vs.* gestational days is as shown. Control embryos (filled triangles, wild-type and heterozygous embryos were pooled together as there were no differences between these two groups) and knockout embryos (filled circles) were as shown. The growth curve showed a linear increase from E9.5 to E19.5 in controls, but deviated at ~E14.5 in *Dhcr7*$^{-/-}$ embryos. Body lengths at E17.5 (18.87 ± 1.29 mm in controls, n = 15 *vs.* 16.69 ± 1.05 mm in *Dhcr7*$^{-/-}$, n = 7, $p < 0.05$), E18.5 (21.35 ± 1.05 mm in controls, n = 15 *vs.* 19.38 ± 0.9 mm in *Dhcr7*$^{-/-}$, n = 5, $p < 0.05$) and E19.5 (23.4 ± 0.97 mm in controls, n = 13 *vs.* 20.3 ± 0.44 mm in *Dhcr7*$^{-/-}$, n = 4, $p < 0.05$) were significantly decreased, compared to those in controls. Results are expressed as mean ± s.d.

littermates. An experienced investigator can pick out knockout pups based on this along with presence of hypoxia and their lack of spontaneous movement. The breathing frequency in P0 Dhcr7$^{-/-}$ pups was markedly slower than control littermates (34 ± 7 breaths/min in Dhcr7$^{-/-}$, n = 10 vs. 92 ± 16 breaths/min in controls, n = 32, $p < 0.001$) and the breathing was observed to be more irregular and shallow, with long periods of apnea.

To determine the gestational stage at which growth of the knockout embryos was affected, embryos were harvested at various stages of gestation and their body lengths compared between *Dhcr7*$^{-/-}$ and controls. A linear increase in body length from E9.5 to E19.5 in control embryos was observed (Fig. 1). No significant differences in body length between wild-type and heterozygous embryos were noted (data not shown). In contrast, knockout embryos showed comparable body length growth until E14.5~E16.5, then began to show a slower increase in length, such that by E17.5, this was statistically significant (18.87 ± 1.29 mm in controls, n = 15 compared to 16.69 ± 1.05 mm in *Dhcr7*$^{-/-}$, n = 7, $p < 0.05$, Fig. 1).

Dhcr7$^{-/-}$ *embryos at late stages displayed pulmonary hypoplasia with delayed saccular development*

Wet lung weights, as well as lung to body weight ratios were significantly lower in *Dhcr7*$^{-/-}$ at E18.5 compared to those in wild-type but not at E13.5 (Table 1). Both body and lung weights were reduced, but lungs seemed to be more affected. A representative figure of embryos at E10.5 and of the pups at birth was shown in Fig. 2A and 2B.

We examined the lungs for any gross morphological abnormalities. The overall organogenesis of lungs was preserved in *Dhcr7*$^{-/-}$ pups; four right lung lobes and a single left lobe flanking the heart were easily seen on external examination at birth (Fig. 2D). Examination for lobation at E13.5 also showed comparable gross anatomy (Fig. 2C) between wild-type and knockout embryos. Histological analyses of the cardiopulmonary structures at E20.5, taken just before birth to avoid artifacts from lack of lung inflation, also confirmed normal gross anatomic development (Fig. 2E and 2F). Additionally, no cardiac defects were identified and this was confirmed by more detailed histological analyses (data not shown). Thus, despite the obvious hypoxia frequently observed at birth of the

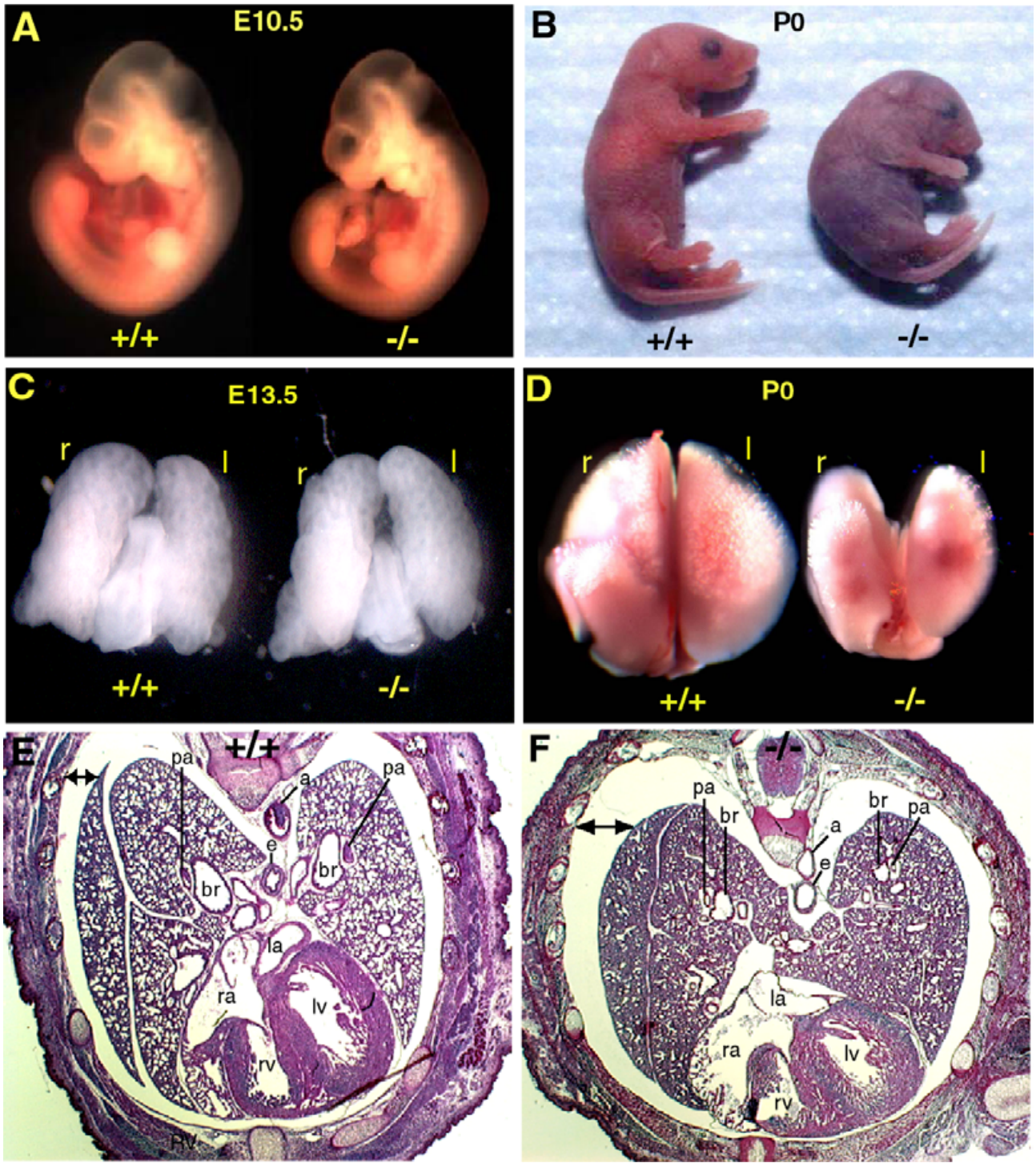

Figure 2

Embryonic size, lung morphology and histology at various stages of development. Panel A shows the size and general morphology of wild-type (+/+) and *Dhcr7*$^{-/-}$ (-/-) embryos at E10.5, without significant difference. At P0, the knockout pups were significantly smaller and appeared hypoxic (panel B). Panel C shows dorsal views of lungs from knockout and wild-type at E13.5 and panel D those at P0. Cross-sectional examination at the cardiopulmonary level at E 20.5 (prior to birth) showed normal lobar septation, but lungs from knockout animals were smaller in size and had less distal sac space (cf. panels E and F). Original magnification: Panels A and C, 2X; panels B and D, 0.7X; E and F, 2X. Labels: r, right; l, left; b, bronchial; br, bronchiole; e, esophagus; pa, pulmonary artery; ra, right atrium; la, left atrium; rv, right ventricle; lv, left ventricle.

knockout pups, major cardiac structural abnormalities were not observed to account for this phenotype.

No distinguishable morphological differences were discernable between *Dhcr7*$^{-/-}$ and wild-type lungs at E10.5, E13.5, E14.5 and E16.5 at low (10X) or high (40X) magnifications (Fig. 3, panel A: a-h, data for E10.5 and E13.5 not shown). However, from E17.5 onwards, lungs from knockout embryos appeared to have less saccular space and relatively more mesenchyme compared to wild-type lungs (Fig. 3, panel A: I-x). Lungs from control animals showed normal progression with formation of sac-like structures, the precursors of the alveoli (Fig. 3, panel A: i, m, q and u). In lungs from knockout embryos, expansion of epithelial tubules occurred but was significantly delayed (Fig. 3, cf. panel A: j, n, r, v with i, m, q and u). Morphometric measurements of lung sections at E17.5, E18.5, E20.5 and in lungs from neonates showed that the proportion of terminal sac space area was significantly decreased in *Dhcr7*$^{-/-}$ lungs, compared wild-type lungs (Fig. 3, panel B). Interstitial mesenchyme appeared thicker and the lungs had less septation compared to control lungs. This 'thickening' of the alveoli may explain the hypoxia frequently seen in *Dhcr7*$^{-/-}$ pups at birth.

Attenuated cell proliferation in late gestational Dhcr7$^{-/-}$ *lungs*

Does the loss of normal cholesterol biosynthesis lead to abnormalities of cell proliferation/division or cell death? Cell proliferation was examined by immunostaining for PCNA and also by BrdU incorporation. Both PCNA and BrdU staining of wild-type and knockout lungs at early gestational stages (E13.5 and E14.5) showed comparable patterns (Fig. 4, panels A-D). However, a clear reduction of PCNA and BrdU labeling was visualized in distal lungs of knockout embryos at late gestational stages (E18.5 and E20.5, Fig. 4, panels E-H). Attenuated PCNA labeling was also noted in knockout hearts at term (Fig. 4, cf. panels I and J). When lungs were stained for pHH3, a marker of active cell division, a clear reduction of pHH3 expression in the epithelium of knockout lung was observed at E20.5 but not at E14.5 (Fig. 4, panels K, L, O and P). In contrast, using the TUNEL assay, no apparent differences in cell apoptosis rates were observed between wild-type and knockout lungs at E18.5 (Fig. 4, cf. panels M and N). Thus, at the late gestational stages, cell proliferation/division was impaired in knockout embryos with no increase in cell death rates.

Sterol content of developing lungs in Dhcr7 *deficient mice*

Markedly elevated 7-DHC/8-DHC levels and reduced body cholesterol levels have been reported previously in *Dhcr7*$^{-/-}$ P0 mice [16,17]. A significant amount of cholesterol was detectable in lungs of *Dhcr7*$^{-/-}$ mice, comprising ~60% and ~30% of total tissue sterols at E13.5 and neonate, respectively. In contrast to the doubling of cholesterol in the lungs of wild type embryos (1.82 mg/g tissue at E13.5 to 3.55 mg/g tissue at P0), cholesterol content in the lungs of *Dhcr7* null embryos remained at almost constant low levels between E13.5 and P0 gestational stages (Fig. 5). There was a progressive increase in 7-DHC and 8-DHC; the latter is generated as a spontaneous isomerization from the former. Total sterols at birth were reduced in lungs of the *Dhcr7* null mice, but were only lower by ~30% (Fig. 5, see values for P0 mice).

Cholesterol is absolutely required for steroid hormone synthesis by the adrenal glands. Adrenal insufficiency, as has been reported in some severe cases of SLOS patients, could be responsible for the lung hypoplasia and perinatal lethality [30]. Steroids, but particularly corticosteroids, are necessary for lung maturation, especially the synthesis and secretion of surfactant components [31]. We determined plasma corticosterone levels in P0 mice within 12 h of birth. Wild type P0 mice had corticosterone levels of 158 ± 50 ng/ml (n = 11), compared with 225 ± 50 ng/ml (n = 7, $p < 0.01$) in *Dhcr7*$^{-/-}$ P0 mice. Thus, the corticosterone levels in *Dhcr7*$^{-/-}$ mice were not decreased, but increased by ~40%. However, since these P0 mice were dying, perhaps this increase was sub-optimal given the stress. Nevertheless, an absolute lack of corticosterone was not present in these knockout pups.

To further rule out any effects of corticosterone deficiency on lung immaturity, we examined lungs for surfactant protein expression. Surfactant protein C, as determined by IHC, was comparable in lung sections from wild-type or *Dhcr7* null embryos at either E18.5 or at E20.5 gestational ages (Fig. 6, panel A). Northern analyses for SP-A, SP-B, SP-C or SP-D showed no significantly differences between wild-type and *Dhcr7* null mice at term (Fig. 6, panel B). Thus, surfactant protein expression was not altered by Dhcr7 deficiency.

Dhcr7$^{-/-}$ *lungs showed abnormal differentiation of type I alveolar epithelial cells (AECs)*

At E20.5, the distal lung of wild type embryos consisted of saccular structures lined by flat type I AECs, and by cuboidal surfactant-producing type II AECs (Fig. 7A). In contrast, the formation of these typical saccules was impaired in Dhcr7 deficient lungs. Instead, these saccular structures were lined by a low columnar epithelium that lacked flattened type I-like cells with the presence of many undeveloped or arrested epithelial tubules (Fig. 7B). Consistent with disruption of type I AECs differentiation was the dramatic reduction of expression of T1α, an apical membrane protein marker of lung type I AECs (Fig. 7, cf. panels C and D). Decreased immunostaining for AQP5, another type I AEC marker, was also noted in Dhcr7 deficient lungs at E20.5, compared to control lungs (Fig. 7, cf.

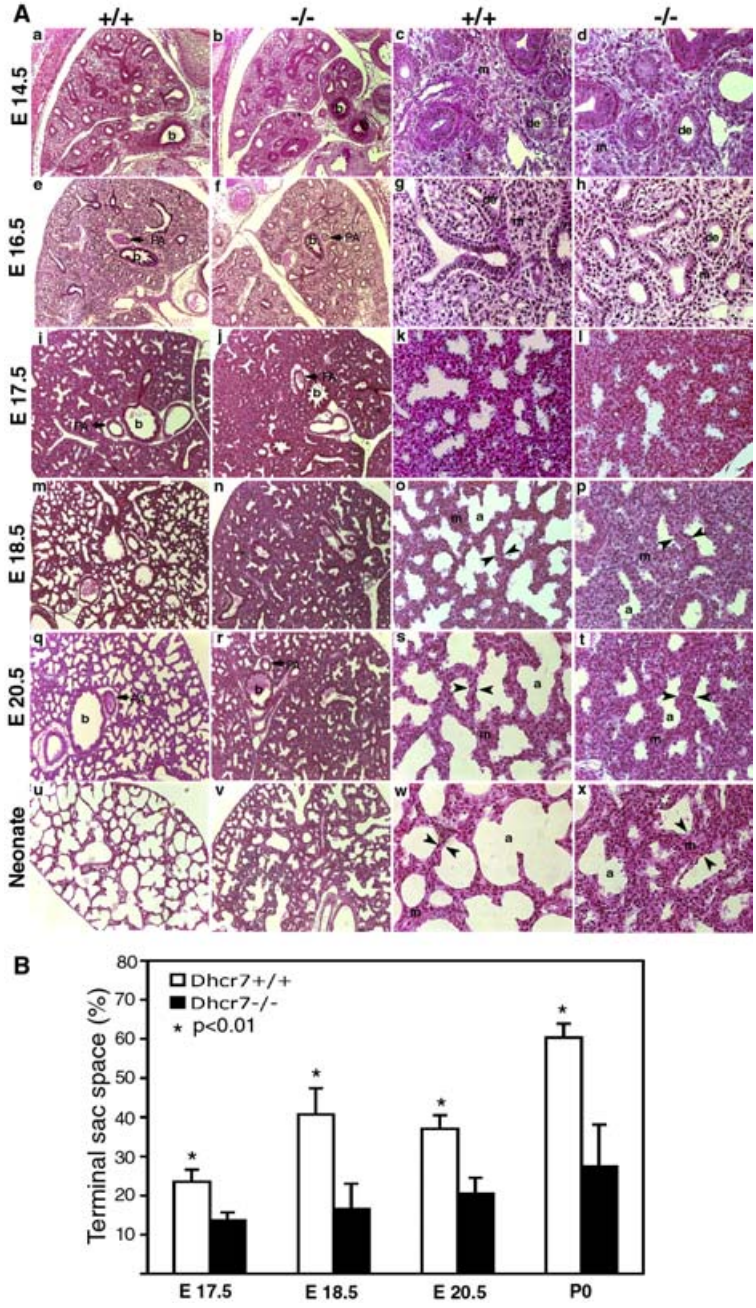

Figure 3

Histological analyses of lungs at various embryonic stages. Panel A indicates lung sections stained with H and E, and taken at various gestational stages as indicated. The first two columns are at lower magnification (10X) and the last two columns at higher magnification (40X). The first and third columns are representative sections from wild-type (+/+) embryos and the second and fourth columns from knockout (-/-) embryos. No differences were visible at E14.5 or E16.5 (panel A, a-h). Significant differences were visible from E17.5 onwards (panel A, i-x). Distal tubules showed dilation and mesenchyme thinning, with progression of septation in wild-type lungs (panel A, i, m and q), whereas the knockout lungs showed less saccular structures and more mesenchyme (panel A, j, n and r). At higher magnifications of wild-type lungs (panel A, k, o and s), developing pre-alveoli and thinning mesenchyme (arrowheads) were seen but sections from knockout embryos showed a delay in this sequence of development (panel A, l, p and t). At birth, lungs from knockout pups showed deficient septation and thick-walled mesenchyme (panel A, x, arrowheads). Labels: de, distal epithelium; m, mesenchyme; PA, pulmonary artery; a, pre-alveoli; b, bronchi. Panel B shows the morphometric analyses of lung terminal sac spaces in lungs at various gestational stages. A significant reduction in the terminal sac space was noted from E17.5 onwards. Results are expressed as mean ± s.d.

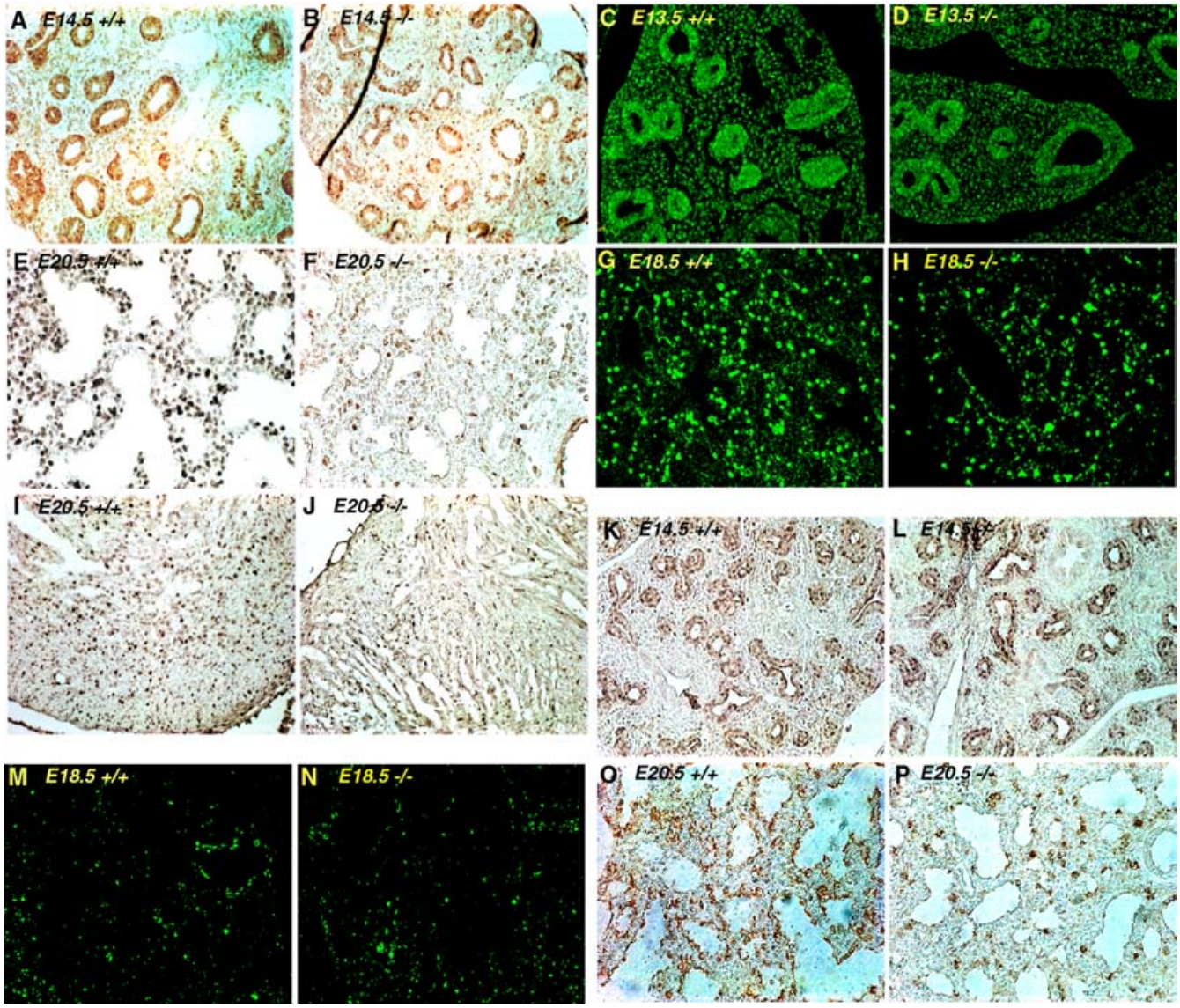

Figure 4

Analyses of cell proliferation, cell division and cell death. Cell proliferation (PCNA: panels A, B, E and F; BrdU: panels C, D, G and H), cell division (pHH3: panels K, L, O and P) and cell death (TUNEL: panels M and N) were analyzed by immunostaining on lung sections at early and late gestational stages. Both PCNA and BrdU labeled cells in both epithelial and mesenchymal regions were comparable at early stages (E14.5 for PCNA and E13.5 for BrdU) between wild-type (+/+) and knockout (-/-) lungs. Positively stained cells in distal lungs at late stage (E20.5 for PCNA and E18.5 for BrdU) from knockout lungs were markedly reduced, compared with wild-type. PCNA labeling of cardiac muscle was also attenuated in knockout embryos at E20.5 (cf. panels I and J). No apparent differences in TUNEL immunostaining were observed in lung sections at E18.5 between wild-type and knockout. The pHH3 immunostaining was comparable between wild-type and knockout lungs at E14.5, and the lungs from wild-type at E20.5 showed a high index of positive cells, whereas lungs from knockout showed a apparent reduced staining pattern. Note the dividing cells are mainly epithelial. Original magnification: A-D and G-N are 20X; E, F, O and P are 40X.

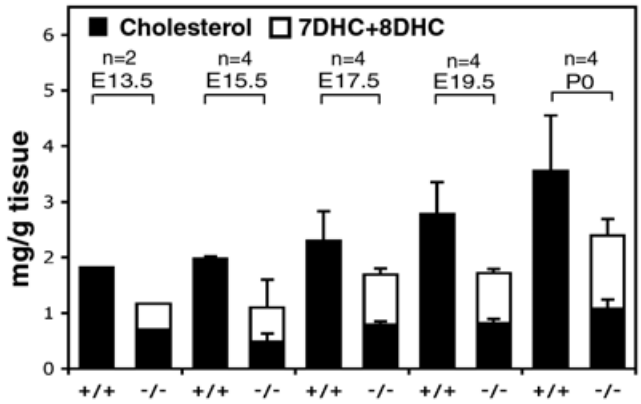

Figure 5

Sterol analyses of embryonic lungs. Sterol contents, including cholesterol (black bars) and 7DHC/8DHC (white bars), were quantitated by GC-MS in the lungs from wild-type (+/+) and knockout (-/-) embryos. Results are expressed as mean ± s.d and the number of lungs analyzed is as indicated. Total sterols were lower at all stages in knockout lungs, with almost no increase in cholesterol content with time (black bars), but there was a progressive increment in the precursor sterols, 7DHC/8DHC (open bars), with increasing gestation.

panels E and F). Megalin, a low density lipoprotein receptor (LDLR) gene family member, is expressed by embryonic epithelial cells and can function as an endocytic Shh receptor [32]. Megalin was highly expressed on the distal epithelium at E20.5 from wild-type lungs, as well as type I AECs lining the developed saccules (Fig. 7G). In contrast, though megalin staining was detected in developing saccules in knockout embryonic lungs, its expression was confined to undifferentiated cuboidal cells (Fig. 7H), further indicating a delay in type I AECs differentiation in the knockout lungs.

Delayed vascular development in Dhcr7$^{-/-}$ *lungs*

There is a close relationship between blood vessel development and lung structural development. At later lung developmental stages, timed capillary bed development is essential for the formation of mature alveolar gas-exchange, with a loss of mesenchyme separating the capillary beds and the AECs [19]. In *Dhcr7*$^{-/-}$ lungs at late gestational stages, the relative abundance of mesenchyme was consistent with the general arrest in sacculation. To investigate whether the delayed lung sacculation also involved abnormal blood vessel development, immunostaining for the α-isoform of caveolin-1 (cav-1α) and platelet endothelial cell adhesion molecular (PECAM-1) were performed on sections from wild-type and *Dhcr7*$^{-/-}$ lungs. In the developing lung, cav-1α is expressed strictly in the endothelium of developing capillary and blood vessels. Cav-1α is present in the terminally differentiated type I AECs, but is not detectable in its progenitors or type II AECs [33]. At E14.5, both the epithelium and mesenchyme were negative for cav-1α staining, and cav-1α was detected in the developing blood vessels and capillaries, with no differences observed between wild-type and *Dhcr7*$^{-/-}$ lungs (Fig. 8, panels A and B). Cav-1α immunostaining demonstrated that the vascular development proceeded rapidly during saccular stages in normal lungs (E17.5 and E20.5). In near-term normal lungs (E20.5), an extensive vascular network, associated with markedly thinned septation walls of well-developed alveoli and close apposition to flat type I AECs, was observed (Fig. 8, panels C and E). In contrast, the cav-1α patterns in lungs from *Dhcr7*$^{-/-}$ embryos revealed a relatively undeveloped pulmonary capillary bed (Fig. 8, panels D and F). At E20.5, cav-1α stained cells in knockout lungs were embedded in a relatively thick mesenchyme surrounding undeveloped epithelial tubules, and these epithelial cells remained cuboidal, instead of flattening out (Fig. 8, panel F). PECAM-1 staining at E20.5 confirmed the delayed lung vascular development at these late gestational stages in Dhcr7 deficient embryos (Fig. 8, cf. panels G and H).

Is the pattern of sonic hedgehog expression or signaling altered in Dhcr7$^{-/-}$ *embryos?*

Shh is critical for normal embryonic development and its autoprocessing, resulting in a cholesterol molecule covalently attached at its C-terminus, is a necessary step for its regulated signaling function [23,34]. Thus, disruption of cholesterol biosynthesis could conceivably disrupt its pattern of distribution and thus affect normal development. To determine whether aberrant expression of Shh contributed to the *Dhcr7*$^{-/-}$ lung phenotype, distribution of Shh in the *Dhcr7*$^{-/-}$ and wild-type lungs was assessed from E10.5 to P0 by IHC using Shh-N peptide antibody. At E10.5, the distribution of Shh was detected in the epithelial cells of lung buds (Fig. 9, left panel: C and D), as well as in the more typical Shh-expressing locations, such as the floor plate, notochord and mid gut (Fig. 9, left panel: A-D). Importantly, no differences between *Dhcr7*$^{-/-}$ and control embryos were noted. Likewise, examination of lung sections from increasing gestational ages through to birth showed no significant differences between wild-type and Dhcr7 deficient tissues. The patterns of staining observed were comparable to those previously reported for Shh in mouse lungs [25].

To further investigate Shh signaling in these embryos, we examined the patterns of expression of Patched (Ptch), a cognate receptor for Shh and one whose expression is also regulated by Shh signaling. The patterns of Ptch in lung sections from various gestational stages were also

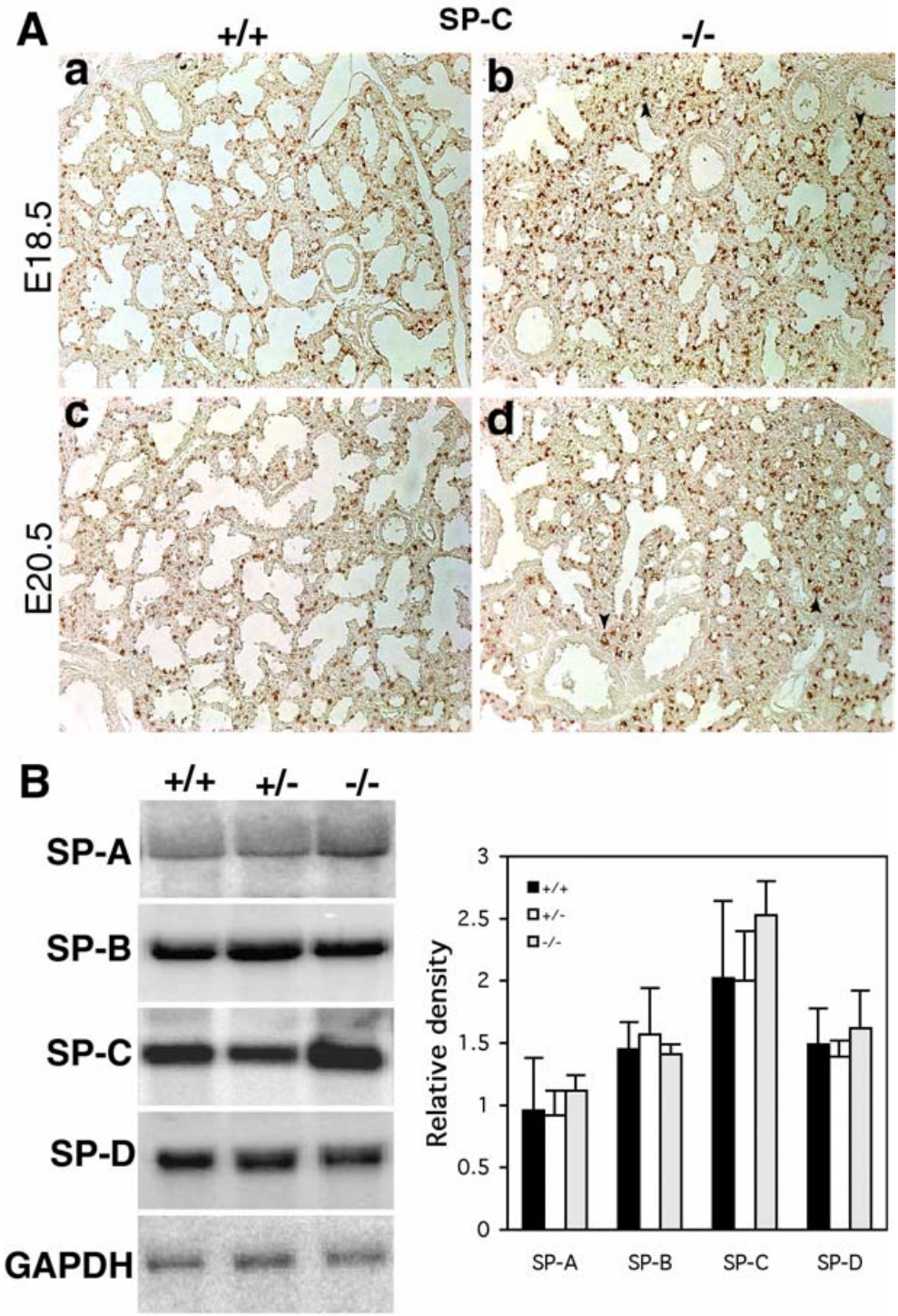

Figure 6

Surfactant protein expression in lungs. Panel A shows the immunostaining patterns for SP-C in lungs at E18.5 and E20.5 from wild-type (+/+) and knockout (-/-) embryos. No significant differences in the patterns of SP-C staining were evident between wild-type and knockout lungs (panel A, a-d). Note that the underdeveloped epithelial tubules in knockout lungs also expressed SP-C (panel A, b and d, arrowheads), indicating normal type II AECs differentiation. Original magnification: 10X. Panel B, left-hand panel, shows a representative result from Northern analyses of total RNA from wild-type, heterozygous and knockout P0 lungs for SP-A, SP-B, SP-C and SP-D expression. Densitometry analyses showed the relative expression (n = 3, mean ± s.d.) of these surfactant protein mRNAs were not significantly different between these three genotypes.

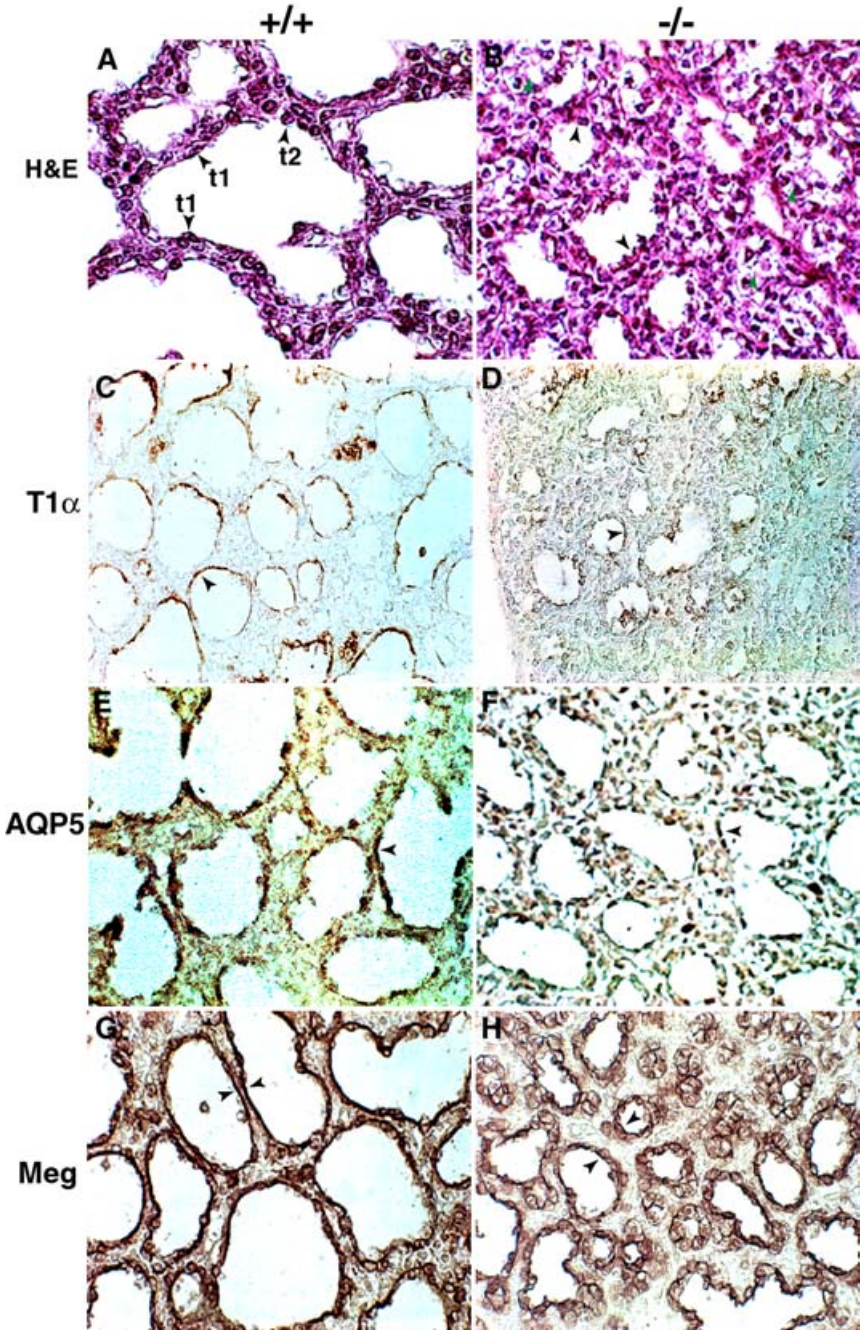

Figure 7

Characterization of type I AECs differentiation. The normal distal saccules of wild-type (+/+) at near term (E20.5) showed typical type I (t1) and type II (t2) epithelial cells (panel A, arrowheads), but knockout (-/-) littermate lungs showed less developed saccules lined by columnar epithelial cells (panel B, black arrowheads), with partially arrested tubules in the distal lung (panel B, green arrowheads). Immunostaining for type I cell markers T1α and AQP5 demonstrated an intense staining in flat epithelial cells in wild-type lungs at E20.5 (panels C and E, arrowheads). In contrast, in knockout littermate lungs, T1α and AQP5 staining was dramatically decreased (panels D and F, arrowheads). Megalin expression (Meg) was detected in the airway epithelial cells, but not in proximal bronchiole epithelial cells (data not shown) in the lungs from both wild-type and knockout at E20.5. The elongated megalin-positive epithelial cells, lining the normally developed sacculi, were readily evident in many areas of the wild-type lungs. In contrast, the terminal epithelial cells positively stained by megalin antibodies in knockout lungs were comprised mainly of undifferentiated cuboidal cells (compare the arrowheads in G and H). Original magnification: A, B, G and H are 60X, C-F are 40X.

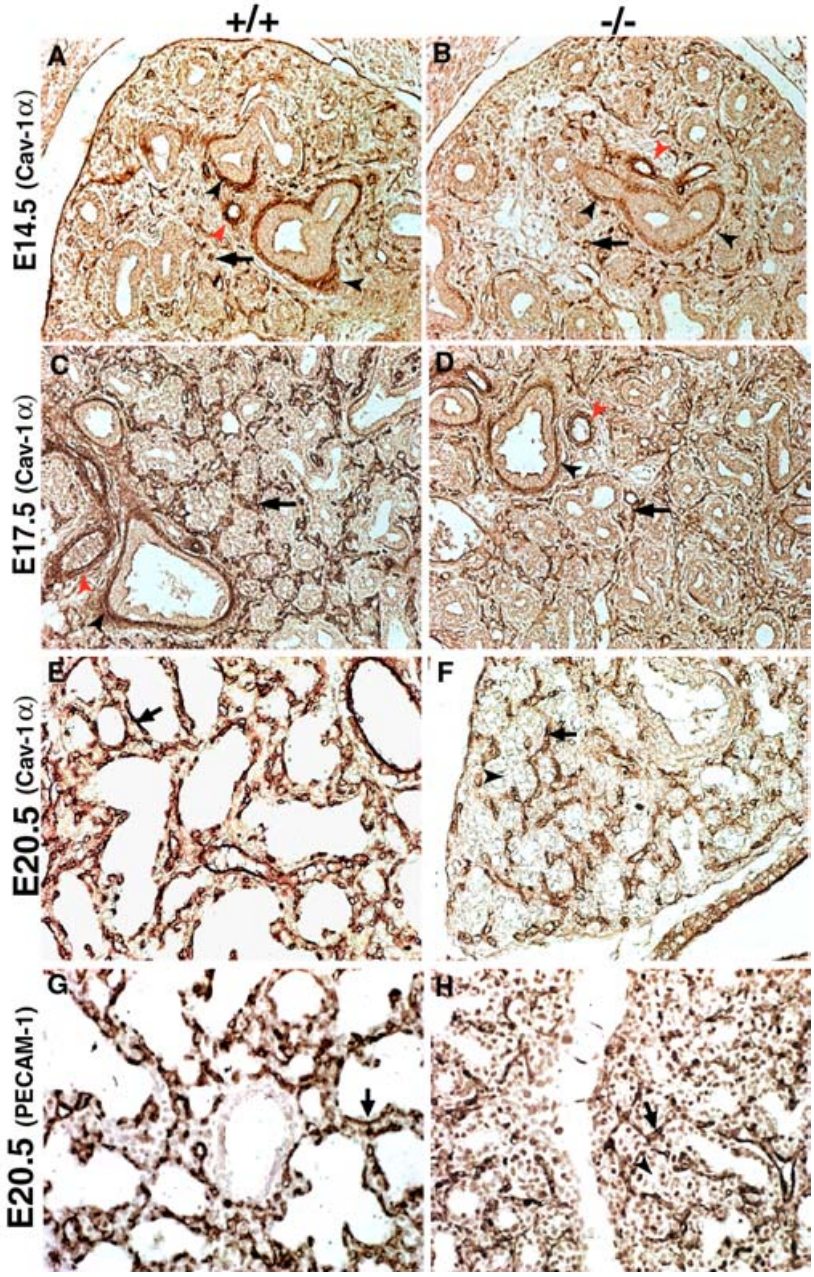

Figure 8

Immunostaining patterns for caveolin-1α and PECAM-1 in lung sections. Cav-1α staining was compared at E14.5, E17.5 and E20.5 stages of development. Both the epithelium and mesenchyme were negative for cav-1α at E14.5. Developing blood vessels (red arrowheads) and capillaries (arrows) (panels A and B) were stained positively for cav-1α, but the staining patterns between wild-type (+/+) and knockout (-/-) lungs were not altered. Cav-1α was also detected at the proximal bronchiole sub-epithelial matrices (panels A-D, black arrowheads). At E17.5, the airway epithelium, negative for cav-1α staining, was surrounded by rings of cav-1α positively stained capillary networks (panels C and D, arrows). Cav-1α expression patterns in lungs from knockout embryos at E17.5 were similar to wild-type embryos, but relative less capillary bed was noted in knockout lungs (cf. panels C and D). At E20.5 of wild-type lungs, both cav-1α and PECAM-1 staining demonstrated an extensive vascular network in the well developed saccules, with staining observed in close proximity to flat epithelial cells lining the air spaces (panels E and G, arrows). However, delayed vascular development was observed in knockout lungs, showing capillaries (panels F and H, arrows) of the knockout lungs at E20.5 were embedded in a relatively thick mesenchyme around the undeveloped epithelial tubules in which the epithelial cells were remained cuboidal (arrowheads). Original magnification: A-D are 20X; E-H are 40X.

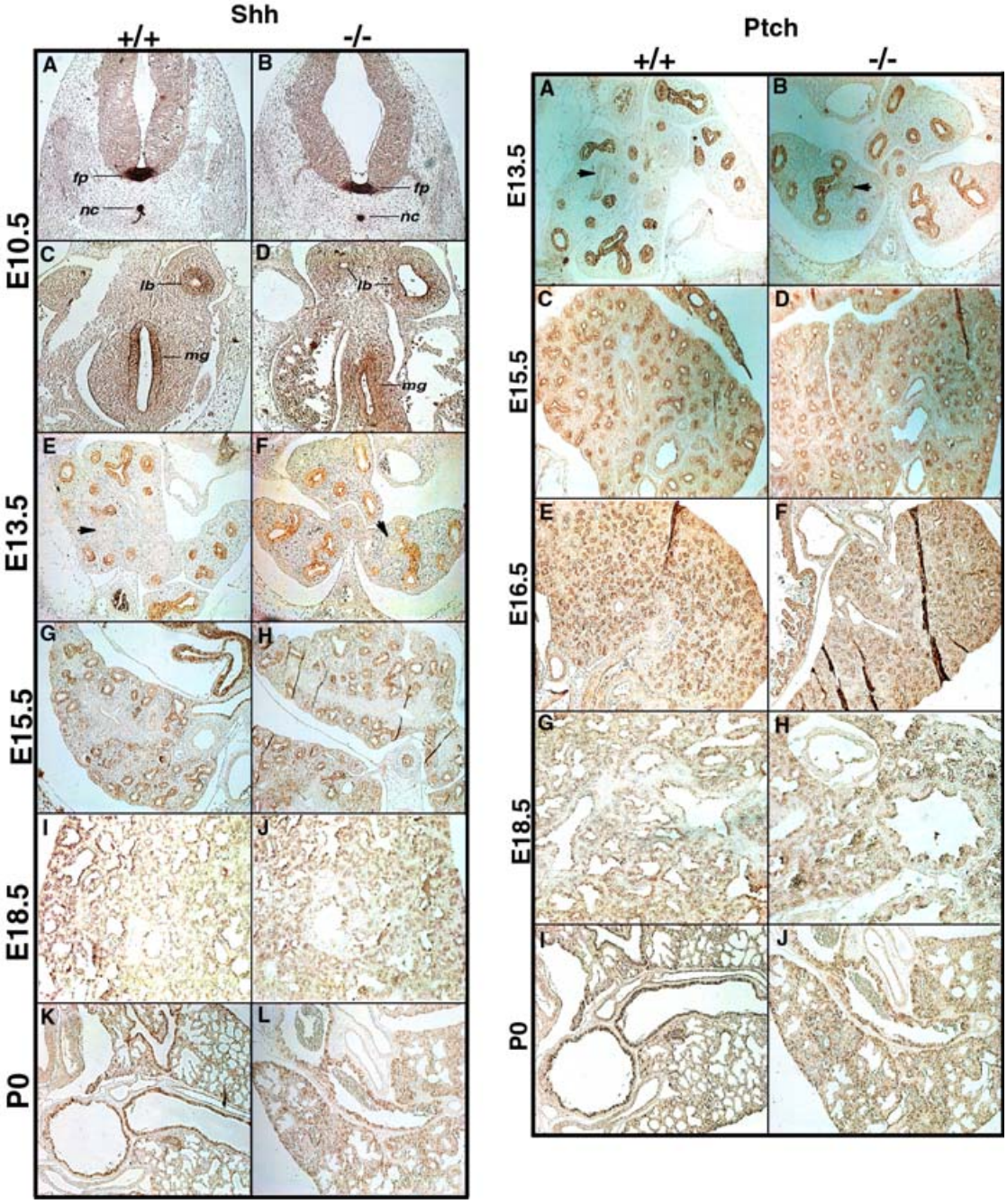

Figure 9

Shh and Ptch expression patterns at different gestational stages in *Dhcr7*$^{-/-}$ and wild-type mice. Left panel shows the Shh immunostaining patterns using an antibody to Shh N-peptide at various gestational stages as indicated by the legend on the y-axis. There were no significant differences noted at any of the stages examined between wild-type (+/+) and knockout (-/-) embryos. At E10.5, Shh was detected in the floor plate (fp), notochord (nc) (A and B), mid-gut (mg) and the epithelial buds of lungs (lb) (C and D). Shh staining was restricted to epithelial cells in the distal region of the primordial tubes of lungs at E13.5 and E15.5. Note that proximal epithelial cells of primordial tubes were not immunostained for Shh (E and F, arrows). Shh was detected in the lung epithelial cells on E18.5, and mainly in the conducting airways in the neonates. Original magnifications: A~H, K and L are 10X, I and J are 20X. Right panel shows the patterns of Ptch IHC at various gestational stages. Immunostaining of Ptch from E13.5 to P 0 confirmed concordance with Shh expression and was not significantly different between wild-type and knockout embryos. Note that the proximal epithelial cells of primordial tubes were also not immunostained for Ptch at E13.5 lungs (arrows). Original magnifications: A~F, I and J are 10X. G and H are 20X.

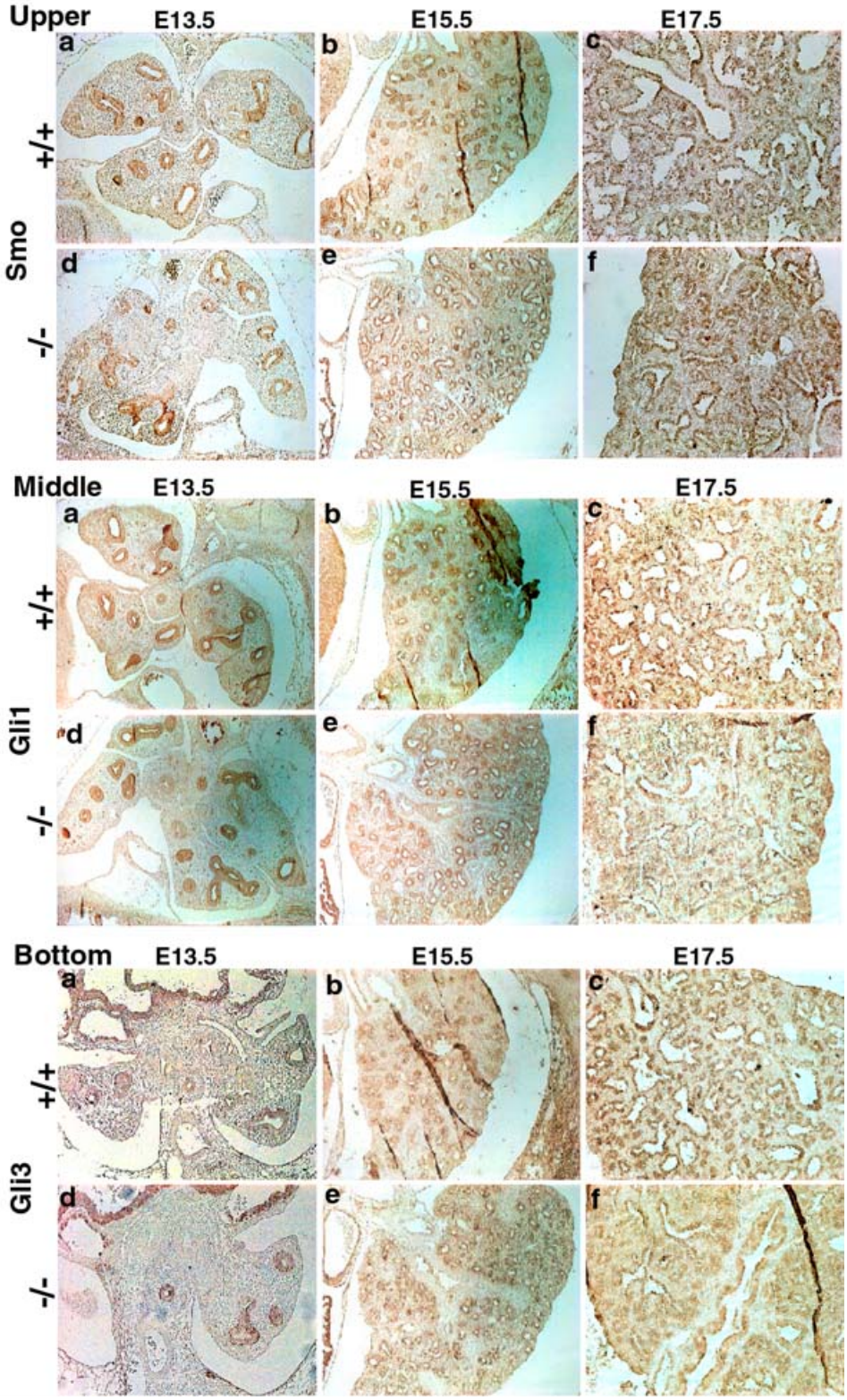

Figure 10

Comparisons of Smo, Gli*1 and* Gli*3* expression in lung sections. Smoothened (Smo, upper panel), Gli1 (middle panel) and Gli3 (bottom panel) showed a pattern of distribution similar to that seen with Shh and Ptch (compare to Fig. 7). No differences between wild-type (+/+) and knockout (-/-) embryos were evident. Original magnifications: 20X.

indistinguishable between wild-type and knockout embryos (Fig. 9, right panels). The expression of Ptch was in concordance with that of Shh (Fig 9, left and right panels), showing lung epithelial cell expression. Downstream of the Shh-Ptch signaling cascade are proteins such as smoothened (Smo), and Gli proteins, key regulators of target-gene expression in response to Shh signaling. No differences in expression patterns for Smo (Fig. 10, upper panels), Gli1 (Fig. 10, middle panels) or Gli3 (Fig. 10, bottom panels) were noted between wild-type and knockout lungs at E13.5, E15.5 and E17.5 gestational days.

Shh protein processing in Dhcr7$^{-/-}$ *embryos*

Since Shh expression, as well as some of the Shh signaling components appeared to be normal in Dhcr7$^{-/-}$ embryos, endogenous autoprocessing of Shh to generate a cholesterol-modified N-terminal fragment of Shh (Shh-Np) was evaluated. COS-1 cells, transfected with full length Shh cDNA (capable of endogenous autocleavage) or a truncated Shh cDNA (Shh-N, expression of the shorter form constitutively) were used as controls (Fig. 11, tracks 1 and 2). Transfection of the full-length cDNA for Shh led to the detection of an ~20 kD protein that corresponds with the cleaved and tailed Shh (Fig. 11, track 1), as previously described [35]. Transfection of COS cells with the constitutive truncated Shh-N cDNA led to two slower migrating bands that correspond to truncated Shh, but which are thought to be generated by differences in lipid modifications, as previously demonstrated [35]. In tissue lysates from wild-type, Dhcr7$^{+/-}$ and Dhcr7$^{-/-}$ embryos at E11.5, a band running at the same position as Shh-Np (autocleaved and tailed) was detected in all of the lysates. There were no distinguishable differences between Dhcr7$^{-/-}$ and the wild-type samples, suggesting that Shh autoprocessing occurred normally, despite an absolute deficiency of cholesterol in knockout embryos. More importantly, no band corresponding to a full-length Shh (~45 kD) was present in the lung lysates from the knockout embryos, suggesting that processing of Shh was not impaired.

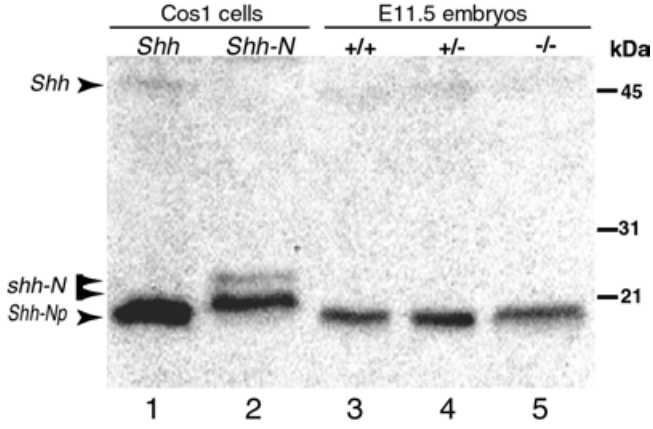

Figure 11

Shh protein autoprocessing in mouse embryos. Western blotting of lysates from wild-type (track 3), heterozygous (track 4) and knockout (track 5) embryos at E11.5, or COS1 cells transfected with Shh (track 1) or Shh-N (track 2) were probed with anti-Shh-N19 antibodies. 20 μg of lysate proteins from Shh transfected COS1 cells and 75 μg from embryos was loaded. Both unprocessed (Shh, upper arrow ~45 kDa, faint signal) and processed (Shh-Np, lowest arrow, strong signal, track 1) forms of Shh were detected from Shh transfected COS1 cells. The two slower migrating bands in Shh-N transfected COS1 cells (track 2) represented Shh-N proteins with different lipid modifications at its N terminus. A major band running at the same position as processed Shh was detected in lysates from all the embryos (tracks 3–5). Importantly, no significant amounts of unprocessed or aberrantly migrating Shh proteins were detected in lysates from knockout embryos at this stage.

Discussion

The elucidation that SLOS is caused by a defect in an enzyme necessary for cholesterol biosynthesis has improved our understanding of embryonic development. This discovery has led to the identification of other disorders of embryonic development caused by mutations in genes encoding other enzymes in the post-squalene steps of cholesterol biosynthesis. Although these genetic studies now implicate the need for normal cholesterol synthesis, the mechanistic role(s) of cholesterol in normal embryonic development remains to be clarified.

In the present study, we report the characterization of lung development in *Dhcr7*$^{-/-}$ embryos. Although cardiac abnormalities are common in human SLOS [36], no structural abnormalities of the heart or the great vessels were observed in the *Dhcr7*$^{-/-}$ pups. Lung development in *Dhcr7*$^{-/-}$ embryos at the early stages, from lung bud formation to canalicular stage, was morphologically similar to controls. Instead, a distinct lung hypoplasia at the saccular stage, characterized by arrested or partially developed distal epithelial tubules, reduced terminal sac space, delayed type I AECs differentiation and delayed vascular development, was consistently observed at late gestational stages in *Dhcr7*$^{-/-}$ embryos. At late stages of normal fetal development, the mammalian alveolar epithelium undergoes an abrupt differentiation as a part of the preparation of the lungs for the postnatal demands of gas exchange [37]. Both type II AECs, producing pulmonary surfactants, and type I AECs, lining the expanded alveoli, are important for alveolar maturation. In addition, the vascular development of alveoli is also essential for normal lung morphogenesis at late gestational stages [19]. We show here that the differentiation of type I AECs but not type II AECs in *Dhcr7*$^{-/-}$ lungs was blocked or delayed, as indicated by

fewer flattened type I cells and by reduced expression of markers of type I AECs, T1α and AQP5. Delayed vascular development was also involved in the delayed sacculation of *Dhcr7*$^{-/-}$ lungs. Additionally, the mesenchyme separating the AECs from the vascular beds remained thickened. In support of normal differentiation of type II AECs, no alteration in the gene expression patterns for surfactant proteins A, B, C or D was noted, nor was the pattern of distribution of SP-C altered in lungs from knockout embryos. Thus, impaired gas exchange, as opposed to poor inflation and alveolar tension, may be the cause of respiratory failure in these pups.

Loss of functional Dhcr7 led to a retardation of embryonic growth from E14.5~E16.5 onwards. By this stage, cholesterol levels were already lower and its immediate precursor, 7-DHC, elevated in the lungs (this study) as well as in the whole body [16,17]. Intrauterine growth retardation (IUGR) followed by postnatal failure to thrive is a universally observed phenotype in SLOS patients [2,18]. We showed here that body length was significantly reduced at later stages of gestation in *Dhcr7*$^{-/-}$ animals, compared to controls. Whole body weights and fresh lung weights (as well as brain, heart and kidney, data not shown) at late gestational stages were also lower in *Dhcr7*$^{-/-}$ embryos. Interestingly, the lower lung/body ratios at E18.5 in *Dhcr7*$^{-/-}$ embryos compared to wild-type suggested a disproportionate inhibition of lung growth than other organs. Cell proliferation and division in *Dhcr7*$^{-/-}$ lungs were markedly arrested without apparent increase in cell apoptosis. Therefore, it appears that growth retardation caused by cholesterol deficiency was primarily because of an inhibition of cell growth and proliferation, rather than an increase in cell death.

Cholesterol is present in *Dhcr7*$^{-/-}$ embryos, as it is in *Sc5d*$^{-/-}$ (lathosterolosis) and *Dhcr24*$^{-/-}$(desmosterolosis) embryos [15,38]. Total sterols and cholesterol in *Dhcr7*$^{-/-}$ embryonic lungs (as well as in brain and liver, data not shown) were reduced and 7DHC/8DHC elevated, but a significant amount of cholesterol was detectable, comprising ~60% and ~30% of total tissue sterols at E13.5 and neonate, respectively. Fetal cholesterol can either be synthesized endogenously in fetal tissues or accrued from extra-embryonic tissues such as maternal serum, placenta, and yolk sac [39]. Since these mice theoretically can not synthesize cholesterol, any accumulation of cholesterol must be derived from the maternal sources. Interestingly, *Dhcr24* null mice are viable but contained almost no cholesterol in plasma and tissues at 3-months, whereas cholesterol content in *Dhcr24* null embryo tissues accounts for ~60% at E11.5 and ~30% at E17.5, of total tissue sterols [38]. These results, as well as this study, suggest that a considerable amount of maternal cholesterol can be transferred to the murine fetus. One explanation of why the *Dhcr24*$^{-/-}$ mice are developmentally normal but *Dhcr7*$^{-/-}$ mice are affected may be because desmosterol can functionally substitute for cholesterol, whereas the other cholesterol precursors can not.

Although a mechanistic understanding of why a deficiency in cholesterol biosynthesis leads to abnormal embryonic development is lacking, a frequently advanced explanation has been that Shh signaling, involved in early developmental patterning, may be disrupted. In the developing lung primordium, Shh is expressed initially at E9 and promotes branching morphogenesis, which is impaired in Shh knockout mice [24], suggesting that Shh, secreted by the epithelium, is critical for branching morphogenesis. In this study, the lack of evidence of abnormal lung branching morphogenesis in the early stages, but a consistent delayed maturation of the gas-exchange region of the lung in the saccular period of development of *Dhcr7*$^{-/-}$ embryos was observed, suggesting early Shh signaling was normal. Shh protein expression and autoprocessing at E11.5 was indistinguishable between wild-type and *Dhcr7*$^{-/-}$ embryos. Additionally, although these experiments were not quantitative, the abundance of Shh appeared unchanged between these genotypes. Thus, it is possible that the cholesterol levels (roughly 50% of normal levels) in *Dhcr7*$^{-/-}$ embryos were enough for completion of Shh autoprocessing or 7DHC accumulated in *Dhcr7*$^{-/-}$ embryonic tissues can also participate efficiently as a sterol adduct in the Shh processing reaction [20]. In this study, we also examined the Shh signaling pathway by immunohistochemistry of known key components of this pathway, such as patched, smoothened and Gli proteins. Shh signaling leads to the activation of transcription and increased protein levels of these components [40-42]. If Shh signaling were defective in *Dhcr7*$^{-/-}$ embryos, these could have resulted in abnormalities of the staining patterns of these components, but no such disturbance was detected. Indeed, the patterns of protein expression seemed comparable and indistinguishable from wild-type embryos at all stages of lung development examined.

In a recent in vitro study [43], mouse embryonic fibroblasts (MEFs) from *Dhcr7*$^{-/-}$ embryos, grown in lipid-depleted culture and transiently treated with cyclodextrin, showed no affect on Shh processing. However, a deficiency in their ability to respond to Shh activation, as judged by reporter gene expression, was demonstrable. In contrast, when CHO cells, that stably expressed Shh, were subjected to sterol deprivation, an arrest of Shh autoprocessing was clearly demonstrable [29]. In the present study, we did not detect unprocessed Shh in *Dhcr7*$^{-/-}$ embryonic tissues at E11.5. Subtle differences in Shh signal transduction can not be excluded by the present study. However, we favor a model whereby the

loss of normal cholesterol biosynthesis is important, not so much for Shh autocleavage, as for the loss of the correct plasma membrane milieu. Since the loss of cholesterol content in the plasma membrane (and perhaps any membrane) is likely to alter the function of receptors more sensitive to this, loss of normal cholesterol synthesis may cause a loss of signal transduction of a host of such pathways. Thus, this effect may not be limited to the Shh pathway and other targets may be more important. This hypothesis is amenable to testing in the *Dhcr7* null mice.

Conclusion

Cholesterol deficiency caused by Dhcr7 deficiency in mice resulted in, along with IUGR, a distinct lung saccular hypoplasia with impaired differentiation of type I but not type II AECs and delayed associated vascular development. Loss of the correct amounts of cholesterol in the membranes may perturb those receptors that depend upon cholesterol for efficient signal transduction. Further investigation of which transcriptional and signal transduction pathways are more significantly affected by the loss of *Dhcr7* will be critical to elucidate the mechanism of lung hypoplasia of this model, as well as the role of cholesterol in embryonic development.

Methods

Animals

All mice were housed in an animal facility at 22°C with a 12 h light ~12 h dark cycle and all protocols were approved by the Institutional Animal Welfare Committee. *Dhcr7* heterozygous animals used in this study have been backcrossed onto a C57BL/6J background for 11 successive generations. The presence of vaginal plugs was considered as embryonic day (E) 0.5. Timed pregnant females were sacrificed, embryos dissected from the uteri and placed in 1X PBS. Crown-rump lengths of the embryos were measured by use of an electronic digital caliper and embryos weighed, after blotting off excess fluid. Each lung was removed intact from the thoracic cavity, blotted free of excess fluid, and weighed. Mice were classified as P0 when birth was witnessed and their breathing activities visualized under a dissecting microscope. Digital images of embryos or lungs were captured using a Zeiss-1000 dissecting microscope. Genotyping was performed by PCR, as described previously [16]. And in selective cases, Southern blotting was performed for confirmation of *Dhcr7* genotype.

Biochemical measurements

Tissue sterol compositions were analyzed by gas chromatography-mass spectrometry (GC-MS) as described previously [2,44]. Serum corticosterone levels were measured by radioimmunoassay (RIA) on the blood obtained from decapitated neonates by a commercial source (DRTC hormone Assay Core Lab, Vanderbilt University, TN).

Histology and Immunohistochemistry

Thoracic parts from embryos or P0 mice were fixed in either Amsterdam's fixative (methanol:acetone:acetic acid:water, 35:35:5:25 v/v) or 4% paraformaldehyde in PBS. Tissues were fixed overnight at room temperature (RT), rinsed in PBS, dehydrated in a graded ethanol series, cleared in toluene and embedded in paraffin. Five μ m sections were mounted on Superfrost-Plus slides (VWR, West Chester, PA) for histological or immunohistochemistry (IHC) analyses.

IHC was performed using an indirect method. After deparaffination in xylene and rehydration through a graded series of ethanol, sections were heated at 95°C in 10 mM sodium citrate (pH 6.0) for an initial 15 min and for three successive 5-min periods [25]. After cooling, the sections were treated with hydrogen peroxide (3% v/v in PBS, pH7.4) for 10 min and rinsed in the PBS. Sections were blocked with 5% normal serum for 2 h, washed in PBS and incubated with antibodies against Shh-N19 (1:100), Patched (1:100), Smo-N19 (1:100), Gli1 (1:100), Gli3-N19 (1:100), SP-C C19 (1:200), caveolin 1α-N20 (1:200), aquaporin 5 (AQP5, 1:200), megalin (1:200), PECAM-1 (1:200) (Santa Cruz Biotechnology, Santa Cruz, CA) or T1α (mAB 8.1.1, 1:1000 dilution, Developmental Studies Hybridoma Bank, Iowa City, IA) overnight at 4° C in a humidified chamber. The sections were washed in PBS, incubated with biotinylated secondary antibodies (1:1000~1:5000, Santa Cruz Biotechnology) in PBS for 2 h at RT, incubated with HRP-streptavidin complex for 30 min, rinsed in PBS and visualized using a Metal Enhanced Diaminobenzidine (DAB) Substrate Kit (Pierce, Rockford, IL). Digital images were collected using a Polaroid Digital Microscope Camera mounted on an Olympus BX40 microscope.

Lung morphometry

Terminal saccular space areas were measured using NIH Image software (NIH, Bethesda, MD) as previously described [45]. Multiple measurements were performed on randomly selected 0.04-mm^2 fields located in the distal part of the lung sections. The proportion of lung comprising terminal saccular spaces was calculated as a percentage of the total examined area of the lung section. Three animals per genotype were examined.

Assessment of cell proliferation/Division/death

Changes in cell proliferation and division were assessed by proliferating cell nuclear antigen (PCNA) IHC, bromodeoxyuridine (BrdU) incorporation and phosphorylated histone H3 (pHH3) IHC. The PCNA (1:2000) and pHH3-Ser28 (1:200) antibodies were obtained from Santa Cruz Biotechnology. For BrdU incorporation, timed pregnant mice at E18.5 were injected intra-peritoneally with 100 μg/gm body weight of BrdU (Sigma, St Louis, MO) 2 h

prior to sacrifice, embryos dissected from uteri and processed as described above. Sections were stained with a monoclonal anti-BrdU antibody (1:100, Developmental Studies Hybridoma Bank, Iowa City, IA) and visualized with a Cy2-conjugated rabbit anti-mouse antibody using a laser-scanning confocal microscope. Cell death was investigated by terminal deoxynucleotidyltransferase-mediated dUTP nick-end labeling (TUNEL) using the Fluorescein In Situ Cell Death Detection Kit (Roche, Indianapolis, IN) according to the manufacturer's protocol.

Western blotting

Sample preparation and western blotting was performed according to Kawakami *et al* with some minor modifications [35]. Briefly, 3 embryos from each genotype were pooled, homogenized in ice cold lysis buffer (50 mM Tris-pH8.0, 150 mM NaCl, 2 mM EDTA, 1% Triton X-100, 0.5 mM DTT, 1 mM PMSF and 2 μg/ml each of aprotinin, leupeptin and pepstatin A) with a tissue homogenizer (PRO Scientific Inc., Oxford, CT) using three pulses of 10 seconds each and then subjected to Dounce homogenizer by 10 strokes. The homogenates were centrifuged at 10,000 g for 30 minutes at 4°C, supernatants collected, protein concentration determined and used for western blotting. COS1 cells were transfected using Superfect transfection reagent (Qiagen, Valencia, CA) with expression constructs encoding either the full-length Shh or the N-terminal fragment of Shh without post-translational modifications (constructs kindly provided by Dr. Pao-Tien Chuang, Cardiovascular Research Institute, University of California, San Francisco, CA), harvested 3 days after transfection and protein extracts prepared as described above. Protein concentration was determined using Bio-Rad protein assay kit (BioRad, Hercules, CA) and 20 μg (COS1 cells) and 75 μg (embryos) of lysates separated by 15 % SDS-PAGE, transferred onto nitrocellulose membrane, incubated with primary antibody (Shh-N19, 1:100) for 2 hours, followed by donkey anti-goat HRP second antibody (1:1000) and visualized by chemiluminescent detection according to manufacturer's protocols (Perkin-Elmer Life Sciences, Boston MA).

Northern blotting

Northern blotting was performed as previously described [46], using total RNA (20 μg) from P0 mice lungs. The cDNA probes for SP-A, SP-B and SP-C were kindly provided by Dr. Jeffery Whitsett (Division of Pulmonary Biology, Cincinnati Children's Hospital Medical Center, Cincinnati, Ohio). A cDNA probe for SP-D was amplified by RT-PCR, using murine SP-D cDNA specific primers (sense 5'-TGCCTGGTCGTGATGGACG-3', and antisense 5'-AGCACTGTCTGGAAGCCCGC-3') and confirmed by sequencing.

Author's contributions

HY designed the experiments. HY, ALP and JLC performed experiments.

GST analyzed tissue sterols by GC-MS and JO performed lung morphometric analyses. HY, AW and SBP analyzed the data. HY and SBP prepared the manuscript. All authors read and approved the final manuscript.

Acknowledgements

We are grateful to Jeffery Whitsett for providing cDNA probes for SP-A, SP-B and SP-C and Pao-Tien Chuang for the Shh and Shh-N plasmids. This research was supported by a Beginning Grant-in-Aid 0160349U from the American Heart Association, Mid-Atlantic Consortium (HY); NIH PO1 HL52813 and NIH PO1 HD39946 (AW) and NIH HL68660 (SBP).

References

1. Simons K, Toomre D, Max Planck Institute for Molecular Cell Biology, Genetics Pfotenhauerstrasse D. Dresden Germany Simons Embl-Heidelberg de: **Lipid rafts and signal transduction.** *Nat Rev Mol Cell Biol* 2000, **1(1):**31-39.
2. Tint GS, Irons M, Elias ER, Batta AK, Frieden R, Chen TS, Salen G: **Defective cholesterol biosynthesis associated with the Smith-Lemli-Opitz syndrome.** *N Engl J Med* 1994, **330:**107-113.
3. Fitzky BU, Witsch-Baumgartner M, Erdel M, Lee JN, Paik YK, Glossmann H, Utermann G, Moebius FF: **Mutations in the Delta7-sterol reductase gene in patients with the Smith-Lemli-Opitz syndrome.** *Proc Natl Acad Sci U S A* 1998, **95:**8181-8186.
4. Wassif CA, Maslen C, Kachilele-Linjewile S, Lin D, Linck LM, Connor WE, Steiner RD, Porter FD: **Mutations in the human sterol delta7-reductase gene at 11q12-13 cause Smith-Lemli-Opitz syndrome.** *Am J Hum Genet* 1998, **63:**55-62.
5. Waterham HR, Wijburg FA, Hennekam RC, Vreken P, Poll-The BT, Dorland L, Duran M, Jira PE, Smeitink JA, Wevers RA, Wanders RJ: **Smith-Lemli-Opitz syndrome is caused by mutations in the 7-dehydrocholesterol reductase gene.** *Am J Hum Genet* 1998, **63:**329-338.
6. Clayton P, Mills K, Keeling J, FitzPatrick D: **Desmosterolosis: a new inborn error of cholesterol biosynthesis.** *Lancet* 1996, **348:**404.
7. Brunetti-Pierri N, Corso G, Rossi M, Ferrari P, Balli F, Rivasi F, Annunziata I, Ballabio A, Russo AD, Andria G, Parenti G: **Lathosterolosis, a novel multiple-malformation/mental retardation syndrome due to deficiency of 3beta-hydroxysteroid-delta5-desaturase.** *Am J Hum Genet* 2002, **71:**952-958.
8. Braverman N, Lin P, Moebius FF, Obie C, Moser A, Glossmann H, Wilcox WR, Rimoin DL, Smith M, Kratz L, Kelley RI, Valle D: **Mutations in the gene encoding 3 beta-hydroxysteroid-delta 8, delta 7-isomerase cause X-linked dominant Conradi-Hunermann syndrome.** *Nat Genet* 1999, **22:**291-294.
9. Derry JM, Gormally E, Means GD, Zhao W, Meindl A, Kelley RI, Boyd Y, Herman GE: **Mutations in a delta 8-delta 7 sterol isomerase in the tattered mouse and X-linked dominant chondrodysplasia punctata. jderry@immunex.com.** *Nat Genet* 1999, **22:**286-290.
10. Grange DK, Kratz LE, Braverman NE, Kelley RI: **CHILD syndrome caused by deficiency of 3beta-hydroxysteroid-delta8, delta7-isomerase.** *Am J Med Genet* 2000, **90:**328-335.
11. Herman GE: **X-Linked dominant disorders of cholesterol biosynthesis in man and mouse.** *Biochim Biophys Acta* 2000, **1529:**357-373.
12. Waterham HR, Koster J, Romeijn GJ, Hennekam RC, Vreken P, Andersson HC, FitzPatrick DR, Kelley RI, Wanders RJ: **Mutations in the 3beta-hydroxysterol Delta24-reductase gene cause desmosterolosis, an autosomal recessive disorder of cholesterol biosynthesis.** *Am J Hum Genet* 2001, **69:**685-694.
13. Konig A, Happle R, Bornholdt D, Engel H, Grzeschik KH: **Mutations in the NSDHL gene, encoding a 3beta-hydroxysteroid dehydrogenase, cause CHILD syndrome.** *Am J Med Genet* 2000, **90:**339-346.

14. Kelley RI, Wilcox WG, Smith M, Kratz LE, Moser A, Rimoin DS: **Abnormal sterol metabolism in patients with Conradi-Hunermann-Happle syndrome and sporadic lethal chondrodysplasia punctata.** *Am J Med Genet* 1999, **83:**213-219.
15. Krakowiak PA, Wassif CA, Kratz L, Cozma D, Kovarova M, Harris G, Grinberg A, Yang Y, Hunter AG, Tsokos M, Kelley RI, Porter FD: **Lathosterolosis: an inborn error of human and murine cholesterol synthesis due to lathosterol 5-desaturase deficiency.** *Hum Mol Genet* 2003, **12:**1631-1641.
16. Fitzky BU, Moebius FF, Asaoka H, Waage-Baudet H, Xu L, Xu G, Maeda N, Kluckman K, Hiller S, Yu H, Batta AK, Shefer S, Chen T, Salen G, Sulik K, Simoni RD, Ness GC, Glossmann H, Patel SB, Tint GS: **7-Dehydrocholesterol-dependent proteolysis of HMG-CoA reductase suppresses sterol biosynthesis in a mouse model of Smith-Lemli-Opitz/RSH syndrome.** *J Clin Invest* 2001, **108:**905-915.
17. Wassif CA, Zhu P, Kratz L, Krakowiak PA, Battaile KP, Weight FF, Grinberg A, Steiner RD, Nwokoro NA, Kelley RI, Stewart RR, Porter FD: **Biochemical, phenotypic and neurophysiological characterization of a genetic mouse model of RSH/Smith--Lemli--Opitz syndrome.** *Hum Mol Genet* 2001, **10:**555-564.
18. Kelley RI, Hennekam RC: **The Smith-Lemli-Opitz syndrome.** *J Med Genet* 2000, **37:**321-335.
19. Warburton D, Schwarz M, Tefft D, Flores-Delgado G, Anderson KD, Cardoso WV: **The molecular basis of lung morphogenesis.** *Mech Dev* 2000, **92:**55-81.
20. Cooper MK, Porter JA, Young KE, Beachy PA: **Teratogen-mediated inhibition of target tissue response to Shh signaling.** *Science* 1998, **280:**1603-1607.
21. Incardona JP, Lee JH, Robertson CP, Enga K, Kapur RP, Roelink H: **Receptor-mediated endocytosis of soluble and membrane-tethered Sonic hedgehog by Patched-1.** *Proc Natl Acad Sci U S A* 2000, **97:**12044-12049.
22. Lewis PM, Dunn MP, McMahon JA, Logan M, Martin JF, St-Jacques B, McMahon AP: **Cholesterol modification of sonic hedgehog is required for long-range signaling activity and effective modulation of signaling by Ptc1.** *Cell* 2001, **105:**599-612.
23. Porter JA, Young KE, Beachy PA: **Cholesterol modification of hedgehog signaling proteins in animal development.** *Science* 1996, **274:**255-259.
24. Pepicelli CV, Lewis PM, McMahon AP: **Sonic hedgehog regulates branching morphogenesis in the mammalian lung.** *Curr Biol* 1998, **8:**1083-1086.
25. Miller LA, Wert SE, Whitsett JA: **Immunolocalization of sonic hedgehog (Shh) in developing mouse lung.** *J Histochem Cytochem* 2001, **49:**1593-1604.
26. Bellusci S, Furuta Y, Rush MG, Henderson R, Winnier G, Hogan BL: **Involvement of Sonic hedgehog (Shh) in mouse embryonic lung growth and morphogenesis.** *Development* 1997, **124:**53-63.
27. Gofflot F, Gaoua W, Bourguignon L, Roux C, Picard JJ: **Expression of Sonic Hedgehog downstream genes is modified in rat embryos exposed in utero to a distal inhibitor of cholesterol biosynthesis.** *Dev Dyn* 2001, **220:**99-111.
28. Gofflot F, Hars C, Illien F, Chevy F, Wolf C, Picard JJ, Roux C: **Molecular mechanisms underlying limb anomalies associated with cholesterol deficiency during gestation: implications of Hedgehog signaling.** *Hum Mol Genet* 2003, **12:**1187-1198.
29. Guy RK: **Inhibition of sonic hedgehog autoprocessing in cultured mammalian cells by sterol deprivation.** *Proc Natl Acad Sci U S A* 2000, **97:**7307-7312.
30. Andersson HC, Frentz J, Martinez JE, Tuck-Muller CM, Bellizaire J: **Adrenal insufficiency in Smith-Lemli-Opitz syndrome.** *Am J Med Genet* 1999, **82:**382-384.
31. Ballard PL, Ning Y, Polk D, Ikegami M, Jobe AH: **Glucocorticoid regulation of surfactant components in immature lambs.** *Am J Physiol* 1997, **273:**L1048-57.
32. McCarthy RA, Barth JL, Chintalapudi MR, Knaak C, Argraves WS: **Megalin functions as an endocytic sonic hedgehog receptor.** *J Biol Chem* 2002, **277:**25660-25667.
33. Ramirez MI, Pollack L, Millien G, Cao YX, Hinds A, Williams MC: **The alpha-isoform of caveolin-1 is a marker of vasculogenesis in early lung development.** *J Histochem Cytochem* 2002, **50:**33-42.
34. Porter JA, Ekker SC, Park WJ, von Kessler DP, Young KE, Chen CH, Ma Y, Woods AS, Cotter RJ, Koonin EV, Beachy PA: **Hedgehog patterning activity: role of a lipophilic modification mediated by the carboxy-terminal autoprocessing domain.** *Cell* 1996, **86:**21-34.
35. Kawakami T, Kawcak T, Li YJ, Zhang W, Hu Y, Chuang PT: **Mouse dispatched mutants fail to distribute hedgehog proteins and are defective in hedgehog signaling.** *Development* 2002, **129:**5753-5765.
36. Lin AE, Ardinger HH, Ardinger R. H., Jr., Cunniff C, Kelley RI: **Cardiovascular malformations in Smith-Lemli-Opitz syndrome.** *Am J Med Genet* 1997, **68:**270-278.
37. Cardoso WV: **Molecular regulation of lung development.** *Annu Rev Physiol* 2001, **63:**471-494.
38. Wechsler A, Brafman A, Shafir M, Heverin M, Gottlieb H, Damari G, Gozlan-Kelner S, Spivak I, Moshkin O, Fridman E, Becker Y, Skaliter R, Einat P, Faerman A, Bjorkhem I, Feinstein E: **Generation of viable cholesterol-free mice.** *Science* 2003, **302:**2087.
39. Woollett LA: **Origin of cholesterol in the fetal golden Syrian hamster: contribution of de novo sterol synthesis and maternal-derived lipoprotein cholesterol.** *J Lipid Res* 1996, **37:**1246-1257.
40. Grindley JC, Bellusci S, Perkins D, Hogan BL: **Evidence for the involvement of the Gli gene family in embryonic mouse lung development.** *Dev Biol* 1997, **188:**337-348.
41. Incardona JP, Gruenberg J, Roelink H: **Sonic hedgehog induces the segregation of patched and smoothened in endosomes.** *Curr Biol* 2002, **12:**983-995.
42. Motoyama J, Liu J, Mo R, Ding Q, Post M, Hui CC: **Essential function of Gli2 and Gli3 in the formation of lung, trachea and oesophagus.** *Nat Genet* 1998, **20:**54-57.
43. Cooper MK, Wassif CA, Krakowiak PA, Taipale J, Gong R, Kelley RI, Porter FD, Beachy PA: **A defective response to Hedgehog signaling in disorders of cholesterol biosynthesis.** *Nat Genet* 2003, **33:**508-513.
44. Tint GS: **Cholesterol defect in Smith-Lemli-Opitz syndrome.** *Am J Med Genet* 1993, **47:**573-574.
45. Zhao J, Chen H, Peschon JJ, Shi W, Zhang Y, Frank SJ, Warburton D: **Pulmonary hypoplasia in mice lacking tumor necrosis factor-alpha converting enzyme indicates an indispensable role for cell surface protein shedding during embryonic lung branching morphogenesis.** *Dev Biol* 2001, **232:**204-218.
46. Wu J, Zhu YH, Patel SB: **Cyclosporin-induced dyslipoproteinemia is associated with selective activation of SREBP-2.** *Am J Physiol* 1999, **277:**E1087-94.